Food Chemistry 487 (2025) 144782

Contents lists available at ScienceDirect

Food Chemistry

journal homepage: www.elsevier.com/locate/foodchem

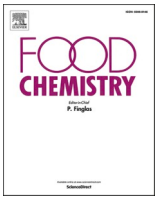

Carbonic or nitrogen maceration of wine grape: Biochemical differences of grape and wine using destructive and non-destructive approach

Alessandro Bianchi [a], Severina Pacifico [b], Gregorio Santini [a], Stefano Pettinelli [a], Gianmarco Alfieri [c], Margherita Modesti [c,*], Andrea Bellincontro [c], Chiara Sanmartin [a], Elisabetta Pittari [d], Simona Piccolella [b], Milena Petriccione [e], Fabio Mencarelli [a], Paola Piombino [d]

[a] Department of Agriculture, Food and Environment, University of Pisa, Via del Borghetto 80, Pisa 56124, Italy
[b] Department of Environmental, Biological and Pharmaceutical Sciences and Technologies, University of Campania Luigi Vanvitelli, Via Vivaldi 43, 81100 Caserta, Italy
[c] Department for Innovation in Biological, Agro-Food and Forest Systems, University of Tuscia, Via De Lellis, 01100 Viterbo, Italy
[d] Department of Agricultural Sciences, Division of Vine and Wine Sciences, University of Naples Federico II, Avellino 83100, Italy
[e] Council for Agricultural Research and Economics (CREA) – Research Centre for Olive, Fruit and Citrus Crops, Via Torrino 3, 81100 Caserta, Italy

ARTICLE INFO

Keywords:
Wine
Grape maceration
Carbon maceration
Nitrogen maceration
HPLC, metabolomics
VOCs
E-nose
NIR-AOFT

ABSTRACT

As an alternative to traditional carbonic maceration (CM), this study explores the use of nitrogen maceration (NM) to create anoxic conditions during winemaking in *Vitis vinifera* cv. Gamay teinturier. A combination of destructive (HPLC, GC–MS, metabolomics) and non-destructive (NIR-AOTF, metallo-porphyrin *E*-nose) methods was used to assess the biochemical effects of CO_2 and N_2 atmospheres. Results show that NM enhances the accumulation of anthocyanins and polyphenols in both grapes and wine, likely due to differences in anaerobic metabolism. VOCs analysis and E-nose evaluation revealed only subtle aroma variations, suggesting sensory equivalence between CM and NM wines. From a sustainability perspective, nitrogen offers advantages in terms of safety, availability, and environmental impact. This dual analytical and environmental perspective supports NM as a viable and innovative technique for producing aromatic, pHenolic-rich wines with reduced ecological footprint.

1. Introduction

Carbonic maceration (CM), a well-known technique used to produce red wine, consists of placing intact grape clusters into a closed tank saturated with carbon dioxide gas (Tesniere & Flanzy, 2011). This treatment has two effects on grapes: first it fills the berry tissue with carbon dioxide, primarily through the stem and stem scar, second,it removes completely oxygen. Why is it important to specify these two actions? Because: i.) carbon dioxide is not an inert gas in term of its interaction with berry cells; ii.) during the treatment, berry cells are no longer exposed to oxygen or nitrogen, gases they are normally in contact with under natural conditions (Paul & Pandey, 2014). During ripening, berry cells are naturally exposed to CO_2 and low or near-zero oxygen levels (Tesniere et al., 2004; Xiao, Rogiers, et al., 2018), leading to a small degree of alcohol formation inside the berry. Plant cells, under low-oxygen (hypoxia) or no-oxygen (anoxia) conditions, adapt their metabolism to compensate for reduced ATP production, shifting from oxidative phosphorylation to anaerobic fermentation (Salvatierra et al., 2020; Wongs-Aree & Noichinda, 2018). This metabolic shift results in the accumulation of fermentation by-products, such as ethanol and CO_2, which can be toxic to cells (Bianchi et al., 2024; Cho et al., 2021; Gibbs & Greenway, 2003; Paul & Pandey, 2014; Pfister-Sieber & Brändle, 1994).

About 78 % of the atmosphere is composed of N_2, dinitrogen gas. However, this vast reservoir of nitrogen is not directly assimilable by living organisms because the N≡N bond is extremely stable and requires substantial energy to break. Plants utilize N_2 in the form of NH^{4+} or

* Corresponding author.
E-mail addresses: alessandro.bianchi@phd.unipi.it (A. Bianchi), severina.pacifico@unicampania.it (S. Pacifico), stefano.pettinelli@phd.unipi.it (S. Pettinelli), gian.alfieri@unitus.it (G. Alfieri), margherita.modesti@unitus.it (M. Modesti), bellin@unitus.it (A. Bellincontro), chiara.sanmartin@unipi.it (C. Sanmartin), elisabetta.pittari@unina.it (E. Pittari), simona.piccolella@unicampania.it (S. Piccolella), milena.petriccione@crea.gov.it (M. Petriccione), fabio.mencarelli@unipi.it (F. Mencarelli), paola.piombino@unina.it (P. Piombino).

https://doi.org/10.1016/j.foodchem.2025.144782
Received 28 March 2025; Received in revised form 5 May 2025; Accepted 14 May 2025
Available online 15 May 2025

NO^{3-} which are typically absorbed through the roots (Bloom, 2015). After harvest, fruit relies on its internal nitrogen reserves until conversion into amino acids occurs (Peerzada Yasir Yousuf et al., 2022). Thus, the response of harvested fruit to a nitrogen-rich atmosphere primarily reflects oxygen deprivation (anoxia), rather than nitrogen assimilation. Short term anoxia (5–15 h) have been shown to stimulate *trans*-resveratrol synthesis in of wine grape (Jiménez et al., 2007), but the effects of longer treatments remain to date unexplored. In contrast, the effects of CO_2-rich environments have been widely explored due to the extensive research on CM (Tesniere & Flanzy, 2011). CM induces several biochemical changes: slight alcohol formation (about 1.5–2 %), reduction of malic acid content by approximately 50 %, and the formation of specific secondary metabolites (Bianchi et al., 2024; Santini et al., 2023). Tesniere and Abbal (2009) reported that "the ability of grape berries to cope with anaerobiosis and initiate AM is mainly related to the characteristics of grapevine (*Vitis vinifera*) alcohol dehydrogenase (*VvADH*)". Surprisingly *VvADH* exhibits high activity in ripe berries, despite the apparent absence of oxygen deficiency. Recent studies (Bianchi et al., 2024; Xiao, Liao, et al., 2018; Xiao, Rogiers, et al., 2018) show that oxygen concentration near grape seeds approaches zero during ripening, explaining the overexpression of *VvADH* and that ethanol diffuses outside during its inner formation. A previous study (Bianchi et al., 2023), comparing CM, nitrogen maceration (NM), and NM/air over 7 days showed increased polyphenol and anthocyanin levels under NM, and slightly higher ethanol content in NM wines.

Additionally, a metabolomic study (Maoz et al., 2019) on table grapes treated with different CO_2 concentration (5, 10, 15 %) and 5 % O_2, confirmed the stimulation of phenylpropanoid pathway and volatile organic compounds (such as ethyl acetate ad diacetyl) under high CO_2 and low O_2.

As clear, the choice of maceration gas thus has significant implications for grape metabolism and wine composition. The monitoring of metabolites formation is generally analyzed through analytical approaches, such as the GC–MS and HPLC. However, in recent years the use of non-destructive techniques has become popular (Bellincontro et al., 2009; Santonico et al., 2010). Among these, near-infrared spectroscopy (NIR) and electronic nose (*E*-nose) have been widely applied in wine and grapes studies. For instance, NIR spectroscopy has been extensively used in wine grapes to monitor metabolite evolution such as phenolic profiling or sugar accumulation (Ferrer-Gallego et al., 2022; Pettinelli et al., 2025; Rouxinol et al., 2022; Rouxinol et al., 2023). Similarly, E-nose systems has been widely utilized for the aromatic characterization of wines (Alfieri et al., 2024; Littarru et al., 2025; Tarì et al., 2024), and often combined with GC–MS and sensory analysis for an holistic approach (Modesti et al., 2024; Pettinelli et al., 2025; Tarì et al., 2024).

In this context, our study focuses on a comprehensive approach combining destructive analyses (HPLC and GC–MS) with metabolomics (UHPLC-ESI-Qq TOF-MS/MS) and non-destructive methods (NIR-AOTF and Me-porphyrins E-nose) to validate our hypothesis: the biochemical effects of anoxia on grapes differ depending on whether the surrounding atmosphere is enriched with CO_2 or N_2.

2. Materials and methods

2.1. Raw materials and maceration/fermentation protocol

Bunches of red grape (*Vitis vinifera* L. cv Gamay teinturier), were hand harvested at Fattoria di Calappiano (Sensi Vigne & Vini, Lamporecchio, Pistoia, Italy). Special care was taken to avoid damage, and only intact bunches were selected—an essential condition for the success of oxygen-free maceration techniques. Immediately after harvest, the grapes were transported to the laboratory of the Department of Agriculture, Food and Environment, University of Pisa (Pisa, Italy) to perform all analytical determinations.

Subsequently, the bunches (about 80 kg) were gently placed intact inside two gas-tight stainless steel tanks, 120 L each, one connected to pure gas carbon dioxide pipeline and the other to pure gas nitrogen pipeline. The two tanks were saturated with pure CO_2 or N_2 from gas tanks provided by SIAD (SIAD Italia, Bergamo, Italy). To ensure the saturation of the tanks with CO_2 or N_2, the inlet valve were connected with a plastic tube touching almost the bottom of the tank; when the tank cap was cloed with grapes nside, the gas valves were opened and slight overpressure was created inside the tank before opening the outlet valve. Both valves were in the cap of the tanks. The outlet valve was connected with a portable gas analyzer (Helpy, Marvil Eng, BZ, Italy). The inlet valve s were cloed when the analyzer measured 0 % O_2. The time of maceration was 8 days at room temperature (18–22 °C). Every two days, tanks were stripped with gas and the atmosphere was analyzed. This procedure was necessary because, in nitrogen gas maceration, CO_2 formation was expected, requiring its removal by means of gas flushing. Indeed, after 2 days, the gas composition was approximately 25 % CO_2 and 74 % N_2. On the fifth (T1) and eighth (T2) days of maceration, grapes were sampled for the analyses. The sampling procedure of bunches consisted in flushing the tank, bottom-up, with gas and rapidly slightly opening the tank cap, sampling bunches, and immediately closing, with continuous gas flushing. At the end of the sampling operation, after closing the tank cap, gas concentration was measured in the headspace and O_2 concentration was 1–2 % which disappeared in 1 h. At the end of maceration (8th day), bunches were removed from the tanks, destemmed and crushed by machine, with dry ice addition; the mass of macerated grapes of each tank was divided in three 20 L glass jars with large opening and inoculated with selected yeasts (Zymaflore Xpure Vin Rouge, Laffort, 33,072, Bordeaux, Cedex-France) at the same room temperature of the maceration treatment. During the fermentation-maceration, *pigeage* (cap punching) was performed once a day (5 min) for 8 days. *Pigeage* was performed alternately, one day in air and the next by flushing nitrogen at the bottom of the jar containing must-wine. At the end of *pigeage*, the plastic cap with an adapted outlet valve was placed back to seal the jar opening. After 17 days, all the jars finished the fermentation, thus the wine was removed from the jars, kept at cold temperature (4 ± 0.5 °C) for 10 days, filtered, bottled and kept in cold room without malolactic fermentation. No sulfites were added.

2.2. Chemical analysis

Harvested grapes (T0) and those collected from maceration jars (T1, T2), were crushed using a juice extractor (JU3701 Frutelia Centrifuge Moulinex, Écully, France), and the resulting musts were centrifuged at 6869 x*g* for 5 min at 22 ± 0.5 °C. The extracted grape juice and the finished wines were analyzed by a calibrated Fourier transform infrared (Wine Scan FT 120, Foss Analytics, Hillerod, Denmark). The instrument was used to quantify key oenological parameters, including: alcohol (% *V*/V); sugars (g/L hexoses), pH, titratable acidity (g/L tartaric acid), volatile acidity (g/L acetic acid), malic acid (g/L), tartaric acid (g/L), citric acid (g/L), lactic acid (g/L), yeast assimilable nitrogen (YAN) (g/L), glycerol (g/L), total anthocyanins (mg/L malvidin), total polyphenols (mg/L gallic acid). Each sample was analyzed in triplicate, with 3 replicates per tank and 3 WineScan measurement per replicate. The accuracy of the Wine Scan reading was validated by destructive analyses performed with traditional OIV methods during the calibration phase, prior to data collection (Bianchi et al., 2021; Pettinelli et al., 2022).

2.3. HPLC polyphenols determination

The comprehensive analysis of polyphenols in grape and wine samples was performed using high-performance liquid chromatography (HPLC) following the method previously reported (Waterhouse et al., 1999). The HPLC consisted of a PU-2089 Plus quaternary pump (Jasco International Co., Ltd., Tokyo, Japan) equipped with a degasser, an AS-2057 Plus autosampler (Jasco International Co., Ltd., Tokyo, Japan) and

a CO-2060 Plus column oven (Jasco International Co., Ltd., Tokyo, Japan). Detection was carried out with an UV-2070 Plus visible detector (Jasco International Co., Ltd., Tokyo, Japan)and data were processed using ChromNAV (software version 2.3). For the analysis, 1 mL of grape juice or wine were diluted 1:1 with phase A, filtered through a 0.45 μm PVDF (Polyvinylidene fluoride) filter, and injected (1 μL) into the HPLC. The separation was carried out with a DionexAcclaim®120 C18 column, 5 μm, 4.6 × 250 mm thermostated at 30 ± 0.5 °C. The mobile phase consisted of a ternary gradient: solvent A = 50 mM ammonium dihydrogen phosphate adjusted to pH 2.6 with acid phosphoric; solvent B = 20 % solvent A and 80 % acetonitrile; solvent C = 0.2 M orthophosphoric acid adjusted to pH 1.5 with NaOH. The solvent gradient used was the same reported in Pettinelli et al. (2024). For qualitative and quantitative assessment of phenolics, calibration curves were prepared using 33 selected standards (Sigma-Aldrich, Steinheim, Germany) chosen to represent major phenolic classes in grape and wine matrices. The phenolic compounds were identified based on their elution order, retention times of standards and UV–Vis spectra characteristics at 520 nm and 280 nm.

2.4. VOCs analysis

The analyses were carried out as recently reported (Bianchi et al., 2025). Briefly, the VOCs extraction was performed by liquid–liquid extraction: 100 mL of wine, spiked with 250 μL of an alcoholic solution of 2-octanol (221 ppm/EtOH) as internal standard, were extracted with 5 mL of CH_2Cl_2 as a solvent. The mix was subjected to magnetic stirring for 1 h at a constant temperature of 21 °C. The emulsion thus obtained was transferred to a separation funnel for 12 h at 4 °C, the organic aromatic extract was finally recovered, dried over Na_2SO_4, and stored at −20 °C until the Gas-Chromatography/Mass Spectrometry (GC/MS) analysis. Each extraction was carried out in triplicate, one each jar. For GC/MS analysis, a GC/MS-QP2010 quadrupole mass spectrometer (Shimadzu, Shimadzu corp., Kyoto, Japan) equipped with a DB-WAX UI column (60 m, 0.25 mm i.d., 0.25 μm film thickness, J&W Scientific Inc., Folsom, CA 95360, USA) was used. Chromatographic conditions and identification procedure were the same already reported in Piombino et al. (2019). The carrier gas was helium (1.3 mL/min), and the temperature program was set as follows: 40 °C for 5 min, raised up to 220 °C at a rate of 2 °C/min, and held for 20 min at the maximum temperature. Electron impact mass spectra were recorded with ion source energy of 70 eV, while the temperature was kept at 230 °C. The peak areas were measured using a GC/MS solution program Shimadzu version 2.30 (Shimadzu corp., Kyoto, Japan). Compounds concentrations were computed as ratio of the response of each compound against the response of the internal standard. The VOC identification was performed by comparison of their retention times with those of pure reference standards under the same chromatographic conditions, as well as by the comparison of experimental mass spectra with those found in the NIST library. In a few cases, the pure chemical standard was not available, and the identified compounds were labelled as tentative (t).

2.5. Metabolomics

2.5.1. Extraction and fractionation

Grape samples were freeze-dried for 5 days using a FTS-System FlexdryTM (SP Scientific, Stone Ridge, NY, USA), and pulverized using a rotary knife homogenizer. Subsequently, the samples underwent ultrasound accelerated maceration (UAM; Branson UltrasonicsTM BransonicTM M3800-E, Germany; 2 cycles, 30 min each) using ethanol (EtOH) with 10 % formic acid (HCOOH) as the extracting solvent (1:5 *w/v*). In order to remove the saccharide component, the alcoholic extracts were subjected to solid phase extraction (Discovery® DSC-18 SPE; Supelco, Bellefonte, PA, USA). According to the manufacturer's guidelines, SPE cartridges were activated with methanol (5 mL) and conditioned with distilled water (15 mL) prior to use. Each sample was eluted first with water and then with methanol, followed by a final wash step with methanol (2 % HCOOH).

2.5.2. UHPLC-ESI-Qq TOF-MS/MS

The methanolic fractions from SPE were analyzed using the Shimadzu NEXERA UHPLC system and the Luna® Omega C18 column (50 × 2.1 mm, 1.6 μm i.d.). The mobile phase consisted of a binary solution A: 1 % HCOOH in H_2O, B: 1 % HCOOH in CH_3CN. The injection volume was 2.0 μL and the flow rate was set at 0.5 mL/min. The separation was performed starting from sol. B at 5 %, it increased to 17.5 % in 5 min, and further increased to 45 % in 2 min, and to 95 % in 1 min, while maintained at 95 % for another 1 min. The initial condition was then restored and column rebalancing was performed. The total analysis time was 15 min. MS analysis was performed using the AB SCIEX TripleTOF® 4600 system (AB Sciex, Concord, ON, Canada) equipped with a DuoSpray™ ion source operating in negative electrospray ionization. The APCI probe was used for automated mass calibration using the Calibrant Delivery System (CDS). The CDS injects a calibration solution corresponding to the ionization polarity and calibrates the mass axis of the TripleTOF® system in all scan functions used (MS and/or MS/MS). The Q-TOF HRMS method, which combines TOF-MS and MS/MS with information-dependent acquisition (IDA), consisted of a full ion scan in the range *m/z* 270–1500 (accumulation time 250 ms) and eight IDA MS/MS scans in the range m/z 100–1350 (accumulation time 100 ms). The MS parameters in negative mode were as follows: curtain gas (CUR) 35 psi, nebulization gas (GS 1) 60 psi, desolvation gas (GS 2) 60 psi, nebulization potential (ISVF) -4.5 kV, interface heater temperature (TEM) 600 °C, declustering potential (DP) -80 V. The applied collision energy (CE) was −45 V with a spread (CES) of 10 V. The instrument was controlled by Analyst® TF 1.7 software, while data processing was performed using PeakView® software.

2.6. E-nose measurements

The E-nose used consists of an array of eight quartz microbalances (QMBs) coated with modified metallo-porphyrins (5,10,15,20-tetraphenylporphyrin, TPP). Their selectivity depends on both the central metal and the peripheral substituents of the macrocycles (Mn-TPP, Co-p-OCH3 TPP, Sn-TPP, Rh-TPP, Co-p-NO2, Cr-TPP, Co-TPP, Ru-TPP) (Di Natale et al., 2007; Mastrangelo et al., 2023). The QMB sensors act as an electromechanical resonator with a natural oscillation frequency (ΔF) of 20 MHz that change when volatiles interact reversibly with its surface. The signal from the sensors was acquired and formatted through software before processing and analysing it (Santonico et al., 2010).

The protocol for the *E*-nose detections was adapted from Martínez-García et al. (2021). 50 mL of wine sample were first degassed by using partial vacuum using a 500 mL Erlenmeyer flask and a Venturi pump system for 1 min. Afterwards, 5 mL of degassed wine were placed in a 10 mL vial and tempered at 25 ± 2 °C for 30 min. The volatiles accumulated in vial headspace were transferred into the E-nose sensor cells using an air stream for 10 min, which was filtered through a trap filled with anhydrous $CaCl_2$. Pure nitrogen (99.99 %) at a constant flow of 100 mL/min was used to clean the sensors for 5 min and the obtained signals were considered as reference for each QMB. Each wine sample was analyzed in three vials and the mean values of each QMB were used for statistical treatment.

2.7. NIR determination

The aim of the analysis with the NIR-AOTF spectrophotometer (Luminar 5030 Miniature Hand-held AOTF-NIR Analyzer, Brimrose, Baltimore, MD) was to evaluate the instrument's ability to discriminate differences among wine samples (Antolini et al., 2021). For the measurement, wine was placed in a test tube in direct contact with the external probe. Measurements were conducted in specular reflectance (R), and the "raw" spectra were acquired in transmittance (T). Spectral

acquisition was performed in the 1100–2600 nm range with a step size of 2 nm and a scan rate of 10 scans/s (Páscoa et al., 2020). Subsequently, the measured spectra were transformed into absorbance values (log 1/T). Each sample underwent the acquisition of 9 spectra, which were then averaged to obtain 3 representative spectra for each sample thesis.

2.8. Statistical analysis

All data were statistically analyzed through the Shapiro-Wilk and Bartlett test to verify normality and homogeneity of variances.

Once these prerequisites were established, data were compared by one-way ANOVA (CoStat, Version 6.451, CoHort Software, Pacific Grove, CA, USA) and Tukey's honestly significant difference (HSD) test with $p < 0.05$ for multiple comparison.

After data acquisition, the numerical data from the NIR-AOTF spectrophotometer and the E-nose were compiled into a matrix for subsequent multivariate statistical analysis to achieve supervised discrimination (pattern recognition). This approach utilized pre-processed data normalized via autoscaling and employed k-means clustering to group samples based on their spectral and sensor response similarities. Cluster centroids were iteratively adjusted to minimize intra-cluster variance, allowing for the identification of natural groupings within the dataset. Statical analyses were performed by using Matlab R2013a (MathWorks®, Natick, MA, USA) PLS Toolbox (Eigenvector Research, Inc., Manson, WA, USA), Past 4.09 (Hammer et al., 2001) and XLSTAT (2020.5) software.

3. Results and discussion

3.1. Chemical characterization of grape at harvest and during maceration

As expected, the first clear observation was the decrease in sugars and the concurrent increase of ethanol during maceration (Table 1). At the end of the maceration phase (8 days), ethanol content in the berries was slightly higher in the N_2 maceration. Compared to the initial grapes, the pH increased in the macerated samples. The formation of glycerol and acetic acid indicates the activation of glyceropyruvic fermentation, likely marking the onset of aerobic fermentation, triggered by post-harvest senescence at room temperature (Imahori, 2024; Pettinelli et al., 2022). As expected, these compounds were detected in both treatments, with increases in both glycerol and volatile acidity (Table 1). A general decrease in Yeast Assimilable Nitrogen (YAN) was observed compared to harvested grapes, particularly in the CO_2 treatment. This marked reduction in YAN reflects intense metabolic activity, likely involving the biosynthesis of nitrogen-based compounds such as enzymes (Pettinelli et al., 2022; Verdenal et al., 2021). The YAN we measured is inorganic nitrogen, thus its use for synthesis of complex forms such as aminoacids or polyamines or even more complex such as enzymes, could explain the decrease but above the difference between CM and NM. CM is a stress situation for grapes stronger than NM because the cell are used to be in a nitrogen atmosphere and in low oxygen during berry ripening as explained in the introduction. Thus, to resist to a stress condition of high CO_2 atmosphere, the berry cell must create an antistress protection by producing the defence system based on enzymes formation and specific metabolites.

Table 1
Chemical characteristics of Gamay teinturier grape at harvest (T0), 5 days of maceration (T1) and the end of maceration (T2, 8 days).

Grape parameters	Units	Harvest (T0)	CO_2 T1	CO_2 T2	N_2 T1	N_2 T2
Alcohol	% V/V	n.d. ^{d}	0.29 ± 0.02 ^{c}	0.66 ± 0.03 ^{b}	0.35 ± 0.04 ^{c}	0.82 ± 0.04 ^{a}
Sugars	g/L hexoses	251.59 ± 0.37 ^{a}	244.85 ± 0.18 ^{b}	235.31 ± 0.22 ^{c}	233.19 ± 0.24 ^{c}	227.31 ± 0.21 ^{d}
pH		3.14 ± 0.02 b	3.36 ± 0.03 ^{a}	3.32 ± 0.02 ^{a}	3.34 ± 0.03 ^{a}	3.32 ± 0.01 ^{a}
Titratable acidity	g/L tartaric acid	7.24 ± 0.03 ^{d}	7.64 ± 0.12 ^{b}	7.72 ± 0.10 ^{ab}	7.42 ± 0.08 ^{c}	7.89 ± 0.09 ^{a}
Volatile acidity	g/L acetic acid	0.05 ± 0.02 ^{d}	0.29 ± 0.01 ^{b}	0.35 ± 0.02 ^{a}	0.24 ± 0.02 ^{c}	0.30 ± 0.03 ^{ab}
Malic acid	g/L	1.20 ± 0.03 ^{a}	1.08 ± 0.03 ^{b}	1.01 ± 0.04 ^{bc}	1.04 ± 0.02 ^{bc}	0.98 ± 0.03 ^{c}
Lactic acid	g/L	0.02 ± 0.01 ^{c}	0.07 ± 0.02 ^{b}	0.13 ± 0.03 ^{a}	0.02 ± 0.01 ^{c}	0.04 ± 0.02 ^{c}
Tartaric acid	g/L	6.02 ± 0.06 ^{a}	5.92 ± 0.05 ^{ab}	5.82 ± 0.06 ^{b}	5.87 ± 0.04 ^{ab}	5.72 ± 0.09 ^{b}
Citric acid	g/L	0.27 ± 0.04 ^{a}	0.24 ± 0.04 ^{a}	0.23 ± 0.03 ^{a}	0.25 ± 0.05 ^{a}	0.23 ± 0.04 ^{a}
YAN	mg/L	281 ± 5 ^{a}	174 ± 10 ^{c}	166 ± 11 ^{c}	261 ± 8 ^{b}	257 ± 10 ^{b}
Glycerol	g/L	n.d. ^{d}	2.66 ± 0.07 ^{c}	3.11 ± 0.04 ^{b}	2.81 ± 0.09 ^{c}	3.35 ± 0.07 ^{a}

Data represent the mean (± SD) of three replicates (bunches) per 1 tank per maceration gas. Different letters within rows indicates significant differences (One way Anova and Tukey post hoc test, $p < 0.05$). n.d. = not detected.

The phenolic profile of grapes (Table 2) highlight metabolic competition between flavonol and anthocyanin biosynthesis, both deriving from the same precursor dihydroflavonol. Although the absolute value differ significantly between flavonols and anthocyanins, they still derives from the same precursor. In grapes subjected to CO_2 maceration at T1 (5 days), a decrease in anthocyanins and an increase in flavonols was observed compared to T0. However, by the end of the maceration (T2, 8 days), both classes showed a decrease. In contrast, under nitrogen maceration, an initial simultaneous decrease in both flavonols and anthocyanins was observed. However, by the end of maceration, both classes showed a significant increase, particularly flavonols. When combining the content of the two compound classes, the total polyphenol content under nitrogen reached approximately 680 mg/L, compared to about 400 mg/L for CO_2 maceration and the initial value at T0 was approximately 600 mg/L. Therefore, CO_2 maceration appeared to reduces flavonol and anthocyanin levels, which might be due to reduced precursor synthesis, particularly hydroxycinnamic acids and/or malonyl-CoA (via the malonic acid pathway) (Amarowicz et al., 2009). This hypothesis is supported by the known acidifying effect of CO_2 on aqueous system (Chidi et al., 2018; Gawel et al., 2020), which may alter the pH and affect enzymatic activity or cause protein through interaction with the amine groups (Ruiz-Capillas & Moral, 2001). This phenomenon is known as the "residual effect" in food preservation (Ruiz-Capillas & Moral, 2001; Viana et al., 2005). Additionally, CO_2, may inhibit cell wall-degrading enzymes by competing with ethylene (de Wild et al., 2003), potentially leading to lower extractability of phenolics during analytical processing. The significant increase in flavonol and anthocyanins observed under N_2, without an inverse trend as expected, is likely due to anaerobic metabolism being more active compared to CO_2 conditions. This is further reflected by higher ethanol and glycerol accumulation and a greater sugars consumption. Although CO_2 treatment also induces oxygen deprivation and accelerates glycolysis, excessive CO_2 concentrations (and consequent oxygen scarcity) may inhibit glycolytic and fermentative pathways, affect ATP production, and lower pH, leading to succinate and/or alanine accumulation (Ke et al., 1995).

The initial decrease in both compound classes could be attributed to stress effects, such as reduced precursor formation due to anaerobic stress conditions, highlighting the necessity of oxygen for polyphenol biosynthesis. The subsequent increase in both classes might result from prolonged stress conditions, leading to heightened activity in the metabolism of hydroxycinnamic acids and the malonic acid pathway, as observed under other stress conditions, such as water stress (Castellarin et al., 2007).

Moreover, the amino acid precursor for hydroxycinnamic acid synthesis, phenylalanine, originates from the shikimic acid pathway, which

Table 2
Single phenolic compounds (mg/L) of Gamay teinturier grape at harvest (T0), 5 days of maceration (T1) and the end of maceration (T2, 8 days).

Phenolic compounds (mg/L)	Harvest (T0)	CO_2 T1	CO_2 T2	N_2 T1	N_2 T2
Cyanidin-3-O-glucoside	14.20 ± 1.31 b	13.19 ± 0.51 b	12.87 ± 0.99 b	17.43 ± 1.04 a	16.60 ± 0.34 a
Delphinidin-3-O-glucoside	102.23 ± 8.91 a	92.19 ± 0.99 a	37.93 ± 1.58 b	37.93 ± 2.31 b	37.94 ± 1.02 b
Peonidin-3-O-glucoside	53.28 ± 3.05 b	50.11 ± 2.01 b	48.71 ± 3.33 b	63.07 ± 3.05 a	64.28 ± 3.54 a
Malvidin-3-O-glucoside	231.04 ± 10.64 c	225.78 ± 4.80 c	173.94 ± 10.42 d	247.21 ± 6.78 b	290.13 ± 7.97 a
Petunidin-3-O-glucoside	8.96 ± 1.01 bc	7.85 ± 1.29 bc	8.51 ± 0.51 c	10.07 ± 0.85 a	9.84 ± 0.66 ab
Total Anthocyanins	**409.70 ± 4.95 ab**	**389.13 ± 1.92 b**	**281.97 ± 3.37 d**	**375.72 ± 2.81 c**	**418.79 ± 2.71 a**
Myricetin	0.09 ± 0.03 c	0.28 ± 0.04 b	0.23 ± 0.04 b	0.34 ± 0.03 a	0.30 ± 0.06 ab
Quercetin	0.75 ± 0.06 a	0.76 ± 0.06 a	0.78 ± 0.06 a	0.75 ± 0.12 a	0.79 ± 0.06 a
Quercetin-3-O-glucoside	2.09 ± 0.12 a	2.30 ± 0.13 a	2.08 ± 0.19 a	2.15 ± 0.18 a	1.22 ± 0.11 b
Quercetin-3-O-rutinoside	3.45 ± 0.69 c	4.01 ± 0.25 c	4.74 ± 0.24 b	5.65 ± 0.32 a	4.05 ± 0.33 c
Quercetin 3-O-ramnoside	0.53 ± 0.12 b	0.80 ± 0.25 a	0.53 ± 0.04 b	0.57 ± 0.06 b	0.64 ± 0.09 ab
Total Flavonols	**6.90 ± 0.21 c**	**8.15 ± 0.15 b**	**8.36 ± 0.11 b**	**9.46 ± 0.14 a**	**6.99 ± 0.24 c**
Procyanidin trimer C1	1.28 ± 0.22 d	3.58 ± 0.44 b	2.85 ± 0.15 c	4.29 ± 0.21 a	3.56 ± 0.04 b
(−)-Epicatechin	188.62 ± 4.39 b	256.63 ± 13.28 a	115.94 ± 8.98 c	109.02 ± 9.76 c	261.41 ± 8.95 a
Procyanidin B3	0.67 ± 0.19 d	2.12 ± 0.07 b	1.74 ± 0.12 c	3.04 ± 0.23 a	0.99 ± 0.05 d
Total Flavanols	**190.56 ± 1.60 b**	**262.33 ± 4.60 a**	**120.53 ± 3.08 c**	**116.35 ± 3.40 c**	**265.96 ± 3.01 a**
(+)-ε-Viniferin	0.65 ± 0.12 b	0.59 ± 0.05 b	1.14 ± 0.07 a	0.66 ± 0.09 b	0.58 ± 0.07 b
Resveratrol	0.16 ± 0.04 a	0.03 ± 0.01 b	0.06 ± 0.03 b	0.05 ± 0.03 b	0.08 ± 0.04 ab
Total Stilbenes	**0.82 ± 0.08 b**	**0.62 ± 0.03 b**	**1.20 ± 0.05 a**	**0.71 ± 0.06 b**	**0.66 ± 0.05 b**
Protocatechuic acid	1.16 ± 0.09 d	1.65 ± 0.19 b	1.21 ± 0.22 cd	1.78 ± 0.45 bc	2.33 ± 0.09 a
Gallic acid	0.57 ± 0.13 b	0.91 ± 0.28 ab	0.61 ± 0.08 b	1.28 ± 0.17 a	0.90 ± 0.04 b
Total Hydroxybenzoic acids	**1.74 ± 0.11 c**	**2.56 ± 0.24 b**	**1.82 ± 0.15 c**	**3.05 ± 0.31 a**	**3.23 ± 0.07 a**

Data represent the means (± standard deviation) of three replicate (bunches) per one tanks per maceration gas. Different letters in each row indicate statistical differences (One way Anova and Tukey post hoc test, $p < 0.05$). n.d. = not detected.

uses phosphoenolpyruvate from glycolysis as a precursor. Under oxygen-deprived conditions (nitrogen), the Krebs cycle halts, glycolysis intensifies, and phosphoenolpyruvate formation increases, consequently boosting shikimic acid and phenylalanine synthesis.

3.2. Metabolomics using UHPLC and HR MS/MS analyses

UHPLC-HRMS analysis of the SPE fractions revealed a metabolic profile dominated by flavonoid-based polyphenols, mainly glycosylated flavonols and anthocyanidins, except for of two *p*-coumaroyl hexoside isomers (2, 3; $C_{15}H_{18}O_8$). Table 3 summarizes the UHPLC-HRMS data, showing tentative identification and relative abundance across time points and treatments (T0, CO_2 T1/T2, N_2 T1/T2), sorted by elution order. Anthocyanins, typically analyzed in positive ion mode, were also successfully detected in negative mode, where $[M\text{-}2H]^-$ ions and their dehydrated species ($[M\text{-}2H + H_2O]^-$) enabled their unambiguous differentiation from flavonol isomers (Fig. S1) (Sun et al., 2012). The identified anthocyanidins varied in both aglycone and saccharide moieties, and compounds sharing the same saccharide residue eluted according to the progressive polarity of their aglycone (delphinidin > cyanidin > petunidin > peonidin > malvidin). Fig. S2 presents the TOF-MS/MS spectra of the hexosyl derivatives 4–6, 8, and 11. Under the experimental conditions used, the precursor ion intensity never exceeded 2–3 %, highlighting the fragmentation pattern of the aglycone ion, which results from the neutral loss of a dehydrated hexose (162/163 Da). This effect is particularly evident when B-ring methoxylation leads to the loss of methyl radicals. As previously noted for flavonols, the ratio between $[aglycone\text{-}H]^-$ and $[aglycone\text{-}H]\bullet^-$ ions serves as an indicator of C-3 glycosylation. Additionally, acylated anthocyanins were tentatively identified. The biosynthesis of these compounds is primarily due by genetic factors of the variety, so much so that some cultivars are not able to produce them due to differences in the expression of genes involved in the acyltransferase activity (Giacosa et al., 2023; Revilla et al., 2017; Rinaldo et al., 2015). Furthermore, as for other polyphenols, environmental factors strongly modify the qualitative-quantitative composition of these compounds (Guan et al., 2016). In particular, compounds 13, 14, 17, 20, 23 and 25 shared an acetyl linked to the hexose sugar. This structural feature was identifiable based on the neutral loss of 204/205 (162/163 + 42) Da from the precursor ion, which provided the corresponding anthocyanidin (Fig. S3). The acyl moiety in compounds 26, 29, 30, 33, and 35 consisted of a p-coumaroyl residue, likely attached to the hydroxymethyl group of the sugar moiety (Fig. S3). In this case, the observed neutral loss was 308/309 Da. Acylation with hydroxycinnamic acid is a well-documented structural modification in most *Vitis vinifera* varieties, contributing to greater colour stability and reduced susceptibility to thermal hydrolysis due to the formation of intramolecular bonds between the anthocyanidin core and the hydroxycinnamic acid residue (Karn et al., 2021). Compounds 19, 21, 22, 27 and 28 presented an additional hexose linked in position C-5 to the aglycone skeleton (Fig. S4), such that in each spectrum the three fragments generated sequentially [M-2H-162 Da]-, [M-2H-162-146 Da]-, [M-2H-162-146-162 Da]- are clearly visible. The base peak is constituted in all cases by the deprotonated aglycone.

Beyond anthocyanins, a B-type procyanidin (1), two glycosylated derivatives of ellagic acid (7, 12) and six flavonols (10, 15, 16, 18, 24 and 34) were also detected. Procyanidin B is a dimer of two (*epi*)catechin units. Previous studies showed that (epi)catechin monomers in grapes are mainly joined through a bond between the C-4 of the first and the C-8 of the second, and that these compounds exert antioxidant, antidiabetic, antimicrobial and cardioprotective properties (Unusan, 2020). MS characterization is based on the recognition of fragments at *m/z* 451.1035, 289.0718 and 425.0878 (accompanied by the dehydration product at *m/z* 407.0772), deriving from the three main fragmentation mechanisms, called Heteocyclic Ring Fission (HRF), Quinone Methide (QM) and Retro Diels Alder (RDA) (Fig. S5) (Formato et al., 2022a).

TOF-MS/MS spectra of the two ellagic acid derivatives showed only the diagnostic fragment ions at *m/z* 300.9989 (98) and 299.9913 (Formato et al., 2022b), formed following the neutral loss of a dehydrated hexose and pentose sugar, respectively. The high resolution MS/MS experiments allowed the latter to discriminate from those formed from quercetin 3-O-hexoside (16), which in the investigated samples is accompanied by the hexuronidyl derivative (15) (Fig. S6). With the same saccharide residue, the other flavonols differed from quercetin by the degree of oxidation and/or methoxylation of the B ring, and were identified as myricetin (10), laricitrin (18) and isorhamnetin 3-O-hexoside (24). Finally, compound 34 was putatively identified as syringetin 3-O-(acetyl)hexoside (Fig. S6). A clear inverse relationship between anthocyanin and flavonol content was observed in the CO_2 T1, CO_2 T2, N_2 T1, and N_2 T2 samples. Compared to T0, flavonol content decreased,

Table 3
UHPLC-HRMS data of compounds tentatively identified in the samples. Each metabolite content is reported as a relative percentage on the sum of compounds' area. RDB = Ring Double Bond; n.i. = not identified.

n.	Rt	Tentative assignment	Formula	$[M-H]^-$ (m/z)	$[M-2H]^-$ (m/z)	$[M-2H+H_2O]^-$ (m/z)	RDB	Error (ppm)	T0	CO_2 T1	CO_2 T2	N_2 T1	N_2 T2
1	1.620	Procianydin B	$C_{30}H_{26}O_{12}$	577.1370			18	3.2	0.16	0.23	0.09	0.01	0.18
2	1.986	*p*-coumaroyl hexoside 1	$C_{15}H_{18}O_8$	325.0928			7	−0.3	0.59	0.12	0.12	0.21	0.18
3	2.216	*p*-coumaroyl hexoside 2	$C_{15}H_{18}O_8$	325.0927			7	−0.6	0.70	0.65	0.24	0.27	0.50
4	2.628	Delphinidin 3-*O*-hexoside	$C_{21}H_{20}O_{12}$		463.0893	481.0993	12	2.4	12.25	10.85	9.92	13.98	11.87
5	3.062	Cyanidin 3-*O*-hexoside	$C_{21}H_{20}O_{11}$		447.0936	465.1042	12	0.7	4.73	5.64	4.80	5.84	5.61
6	3.416	Petunidin 3-*O*-hexoside	$C_{22}H_{22}O_{12}$		477.1049	495.1151	12	2.2	7.60	7.43	8.04	8.42	8.61
7	3.603	Ellagic acid hexoside	$C_{20}H_{16}O_{13}$	463.0524			13	1.3	2.23	2.58	2.41	2.00	2.28
8	3.908	Peonidin 3-*O*-hexoside	$C_{22}H_{22}O_{11}$		461.1093	479.1200	12	0.8	2.69	3.17	2.94	2.98	3.11
9	4.097	Malvidin hexoside	$C_{23}H_{24}O_{12}$		491.1202	509.1306	12	1.4	2.88	1.32	0.41	0.00	0.00
10	4.152	Myricetin 3-*O*-hexoside	$C_{21}H_{20}O_{13}$	479.0836			12	1.0	18.95	11.87	9.90	11.74	10.91
11	4.209	Malvidin 3-*O*-hexoside	$C_{23}H_{24}O_{12}$		491.1193	509.1306	12	−0.4	3.00	4.27	4.87	4.36	5.68
12	4.589	Ellagic acid pentoside	$C_{19}H_{14}O_{12}$	433.0420			13	1.7	1.41	1.83	1.60	1.10	1.45
13	4.660	Delphinidin 3-*O*-(acetyl)hexoside 1	$C_{23}H_{22}O_{13}$		505.0998	523.1098	13	2.0	0.00	0.00	0.00	1.79	0.00
14	4.749	Delphinidin 3-*O*-(acetyl)hexoside 2	$C_{23}H_{22}O_{13}$		505.1000	523.1099	13	2.4	2.91	2.97	2.86	1.78	2.72
15	5.014	Quercetin 3-*O*-glucuronide	$C_{21}H_{18}O_{13}$	477.0685			13	2.2	1.78	1.85	1.58	0.00	0.89
16	5.069	Quercetin 3-*O*- hexoside	$C_{21}H_{20}O_{12}$	463.0890			12	1.7	1.64	1.50	1.34	0.84	0.78
17	5.263	Cyanidin 3-*O*-(acetyl) hexoside	$C_{23}H_{22}O_{12}$		489.1048	507.1151	13	1.9	3.53	3.59	4.08	4.85	3.71
18	5.279	Laricitrin 3-*O*- hexoside	$C_{22}H_{22}O_{13}$	493.1003			12	3.1	3.31	2.69	1.89	1.73	2.00
19	5.333	Delphinidin-3-*O*-(6-*p*-coumaroyl) hexoside-5-*O*-hexoside	$C_{36}H_{36}O_{19}$		771.1782	789.1881	19	0.5	0.95	0.00	0.89	0.90	1.15
20	5.538	Petunidin 3-*O*-(acety)hexoside	$C_{24}H_{24}O_{13}$		519.1159	537.1264	13	2.9	2.78	2.97	3.37	2.52	3.23
21	5.768	Cyanidin 3-*O*-(6-*p*-coumaroyl) hexoside −5-*O*- hexoside	$C_{36}H_{36}O_{18}$		755.1852	773.1921	19	3.1	0.04	0.03	0.03	0.04	0.04
22	5.902	Petunidin 3-*O*-(6-*p*-coumaroyl) hexoside −5-*O*-hexoside	$C_{37}H_{38}O_{19}$		785.1935	803.2040	19	0.4	0.09	0.09	0.12	0.11	0.13
23	6.021	Peonidin 3-*O*-(acetyl) hexoside	$C_{24}H_{24}O_{12}$		503.1205	521.1304	13	2.0	0.83	1.01	1.18	1.04	0.95
24	6.099	Isorhamnetin 3-*O*- hexoside	$C_{22}H_{22}O_{12}$	477.1050			12	2.4	0.35	6.45	6.92	7.43	7.60
25	6.146	Malvidin 3-*O*-(acetyl)hexoside	$C_{25}H_{26}O_{13}$		533.1312	551.1421	13	2.1	3.53	4.16	5.28	3.70	4.04
26	6.233	Delphinidin 3-*O*-(6-*p*-coumaroyl) hexoside	$C_{30}H_{26}O_{14}$		609.1264	627.1353	18	2.3	6.26	5.73	6.03	5.66	6.18
27	6.267	Peonidin 3-*O*-(6-*p*-coumaroyl) hexoside −5-*O*- hexoside	$C_{37}H_{38}O_{18}$		769.1966	787.2115	19	−2.5	0.04	0.06	0.06	0.03	0.04
28	6.293	Malvidin 3-*O*-(6-*p*-coumaroyl) hexoside −5-*O*- hexoside	$C_{38}H_{40}O_{19}$		799.2085	817.2191	19	−0.8	0.12	0.21	0.17	0.12	0.21
29	6.573	Cyanidin 3-*O*-(6-*p*-coumaroyl) hexoside	$C_{30}H_{26}O_{13}$		593.1314	611.1414	18	2.3	1.84	1.83	2.24	2.61	2.01
30	6.684	Petunidin 3-*O*-(6-*p*-coumaroyl) hexoside	$C_{31}H_{28}O_{14}$		623.1426	641.1520	18	3.2	4.76	4.90	6.28	4.96	5.47
31	6.752	n.i.	$C_{38}H_{42}O_{19}$	801.2253			18	0.7	0.58	0.65	0.70	1.01	0.65
32	6.819	n.i.	$C_{24}H_{24}O_{14}$	535.1105			13	2.2	0.28	0.82	0.00	0.00	0.00
33	6.987	Peonidin 3-*O*-(6-*p*-coumaroyl) hexoside	$C_{31}H_{28}O_{13}$		607.1457	625.1565	18	1.5	1.05	1.20	1.72	1.56	1.28
34	6.989	Siringetin 3-*O*-(acetyl)hexoside	$C_{25}H_{26}O_{14}$	549.1261			13	2.0	0.47	0.55	0.00	0.00	0.00
35	7.045	Malvidin 3-*O*-(6-*p*-coumaroyl) hexoside	$C_{32}H_{30}O_{14}$		637.1574	655.1674	18	1.8	5.66	6.79	7.93	6.39	6.51

with myricetin as the most abundant aglycone (Table 3), while anthocyanins increased (Table S1) confirming the aforementioned competition between the two class of polyphenols, having the same precursor. Among anthocyanins, hexosyl derivatives (31–36 %) were the most abundant, followed by *p*-coumaroyl (20–24 %) and acetyl derivatives (14–17 %), while diglycosylated and acylated forms accounted for 0.4–1.6 % (Table S1). Summarizing the percentage values, which is not absolutely correct but just as indication, N_2-treated samples showed higher anthocyanin content than CO_2-treated grapes above all already after 5 days, while in CO_2-treated samples, the highest anthocyanin levels were observed at the end of the process (Table S1). This is in contrast what observed in HPLC with. In UHPLC and TOF-MS/MS we reported the relative percentage and we sum all the compounds while in HPLC we measured only one type of specific anthocyanin.

3.3. Chemical characterization of the wine

Concerning the chemical characterization of the final wines (Table 4), CO_2 increased alcohol content, pH, volatile acidity, glycerol,

Table 4
Chemical parameters of wines at the end of alcoholic fermentations.

Wine parameters	Units	CO_2 wine	N_2 wine
Alcohol	% V/V	13.01 ± 0.08 *	12.56 ± 0.09
Sugars	g/L hexoses	3.09 ± 0.12	3.52 ± 0.09 *
pH		3.55 ± 0.02 *	3.48 ± 0.01
Titratable acidity	g/L tartaric acid	7.78 ± 0.05	8.01 ± 0.08 *
Volatile acidity	g/L acetic acid	0.30 ± 0.02 *	0.23 ± 0.02
Tartaric acid	g/L	5.27 ± 0.06	5.50 ± 0.04 *
Malic acid	g/L	1.80 ± 0.06 *	1.65 ± 0.04
Lactic acid	g/L	0.44 ± 0.04 *	0.27 ± 0.03
Citric acid	g/L	0.22 ± 0.02	0.19 ± 0.03
Glycerol	g/L	8.92 ± 0.06 *	8.50 ± 0.07
Total anthocyanins	mg/L malvidin	1217 ± 42	1481 ± 21*
Total polyphenols	mg/L gallic acid	2525 ± 47	2832 ± 66*

Data represent the means (± standard deviation) of the wine samples from 3 bottles. * = Asterisk in the row of each compound refer to significant differences (Tukey, $p < 0.05$). n.d. = not detected.

malic and lactic acid compared to N_2 wine. On the contrary, N_2 increased residual sugars, titratable acidity, tartaric acid and phenolic compounds (total anthocyanins and total polyphenols) thus confirming what already observed in grapes and in previous study (Bianchi et al., 2023).

The higher content of flavonols and anthocyanins observed in grapes macerated under N_2 compared to CO_2-macerated ones, persisted throughout fermentation and therefore in the final wines, as shown in Table 5. Moreover, flavanols and stilbenes were significantly higher in N_2 wines. For the other compounds, no significant differences were observed.

3.4. VOCs characterization

Table 6 shows the 51 volatile compounds, grouped in chemical classes (namely esters, alcohols, acids, furans, carbonyl compounds, and three miscellaneous VOCs) detected in the wines.

The level of esters, alcohols and acids, the main fermentative-related metabolites, suggest a limited impact of the two types of maceration on the pattern of fermentative VOCs, with total class variation around 5 %.

Among esters, ethyl butanoate, ethyl lactate, ethyl decanoate, and ethyl acetate increased from a minimum of 13 % to a maximum of 34 % in the wines macerated under N_2. On the other hand, Isoamyl acetate, ethyl methyl succinate, methyl and ethyl hydrogen succinate were more abundant in CO_2 wine. Overall, when considering esters most relevant to fruity aroma vectors, namely ethyl butanoate, ethyl hexanoate, ethyl octanoate, ethyl decanoate, ethyl 2-methylbutanoate, ethyl 3-methylbutanoate, ethyl hydroxybutyrate, isoamyl acetate, isobutyl acetate (Ferreira et al., 2022), only ethyl butanoate and isoamyl acetate showed significant differences in the wines. This suggest that the fruity character of a wine produced with N_2 maceration could be comparable to the one obtained with the classical CO_2 maceration. Alcohols, known for their masking effect on fruity esters (Cameleyre et al., 2015), and acids, which act synergistically to enhance fruitiness (San-Juan et al., 2011), also showed only minor differences between the two wines.

Considering the other VOCs classes, significant differences were observed for carbonyl and miscellaneous compounds, but not for furans. Specifically, N_2 wine differs from CO_2 sample for the significant higher amount of furfural and acetoin, with an increasing trend also for

Table 5
Single phenolic compounds (mg/L) Gamay teinturier in the two wine (CO_2 maceration and N_2 maceration).

Phenolic compounds (mg/L)	CO_2 wine	N_2 wine
Cyanidin-3-O-glucoside	26.13 ± 2.10	37.26 ± 2.67 *
Delphinidin-3-O-glucoside	187.89 ± 12.41	261.23 ± 12.12 *
Peonidin-3-O-glucoside	130.84 ± 7.12	171.75 ± 8.19 *
Malvidin-3-O-glucoside	760.96 ± 4.86	945.01 ± 7.93 *
Petunidin-3-O-glucoside	94.20 ± 3.56	103.61 ± 3.76 *
Total Anthocyanins	**1200.01 ± 6.01**	**1518.85 ± 6.94** *
Myricetin	4.82 ± 0.99	9.40 ± 0.77 *
Quercetin	7.59 ± 0.34	8.29 ± 0.20 *
Quercetin-3-O-glucoside	2.56 ± 0.19	16.79 ± 0.81 *
Quercetin-3-O-rutinoside	5.93 ± 0.49	9.14 ± 1.02 *
Quercetin 3-O-ramnoside	2.60 ± 0.11	5.14 ± 0.71 *
Total Flavonols	**23.50 ± 0.84**	**48.75 ± 0.70***
(−)-Epicatechin	820.83 ± 9.39	1116.69 ± 24.91*
Procyanidin B1	21.49 ± 1.42	23.33 ± 0.92
Total Flavanols	**842.32 ± 5.41**	**1140.02 ± 12.92** *
(+)-ε-viniferin	3.41 ± 0.09	3.58 ± 0.29
t-Rasveratrol	1.47 ± 0.13 *	1.10 ± 0.06
Resveratrol	0.65 ± 0.18	1.63 ± 0.31 *
Total Stilbenes	**5.53 ± 0.13**	**6.31 ± 0.22** *
Gallic acid	51.76 ± 7.66	53.65 ± 1.20
Total Hydroxybenzoic acids	**51.76 ± 7.66**	**53.65 ± 1.20**

Data represent the means (± standard deviation) of the wine samples from 3 bottles. * = Asterisk in the row of each compound refer to significant differences (Tukey, $p < 0.05$).

Table 6
VOCs detected in the two wine (CO_2 maceration and N_2 maceration). Compound concentrations are reported semi quantitatively as IS equivalents in μg /L.

Concentration (μg/L)	CO_2 wine	N_2 wine
Esters		
Ethyl butanoate	161.27 ± 1.18	215.91 ± 8.76 *
Ethyl 2-methylbutanoate	6.70 ± 0.01	5.61 ± 0.54
Ethyl 3-methylbutanoate	3.57 ± 0.10	3.66 ± 0.43
Isoamyl acetate	339.01 ± 10.72 *	296.71 ± 2.58
Ethyl hexanoate	166.31 ± 6.37	183.29 ± 1.64
Ethyl pyruvate	27.03 ± 0.31	26.82 ± 2.22
Ethyl lactate	485.34 ± 5.75	546.17 ± 1.19 *
Ethyl octanoate	147.76 ± 6.54	156.30 ± 1.38
Ethyl 3-hydroxybutanoate	89.54 ± 1.12	89.78 ± 1.37
Ethyl 2-hydroxyhexanoate	82.90 ± 0.44	88.83 ± 2.17
Ethyl methyl succinate	5.68 ± 0.54 *	3.88 ± 0.15
Ethyl decanoate	34.05 ± 1.69	40.19 ± 0.99 *
Diethyl succinate	570.50 ± 21.40	531.42 ± 9.30
Ethyl Acetate	57.75 ± 2.67	71.33 ± 0.14 *
β-Phenethyl acetate	26.26 ± 1.37	24.25 ± 0.89
Ethyl 3-hydroxyhexanoate	10.53 ± 1.20	7.72 ± 0.86
Methyl hydrogen succinate	8.49 ± 1.29 *	tr
Ethyl hydrogen succinate	3802.25 ± 8.22 *	3458.35 ± 97.72
Total Esters	**6024.95**	**5750.24**
Alcohols		
2-Methyl-1-propanol (Isobutyl alcohol)	4616.31 ± 333.97	4061.46 ± 89.00
1-Butanol	35.53 ± 2.27	30.67 ± 1.19
3-Methyl-1-butanol (Isoamyl alcohol)	56,189.86 ± 3362.65	52,787.96 ± 1266.16
3-Methyl-3-buten-1-ol	5.67 ± 0.57	5.02 ± 0.55
2-Hexanol	3.26 ± 0.42	3.53 ± 0.03
4-Methyl-1-pentanol	20.81 ± 0.72	27.92 ± 0.44 *
3-Methyl-1-pentanol	74.27 ± 0.91	94.18 ± 2.09 *
1-Hexanol	426.95 ± 9.57	464.35 ± 2.86 *
3-Ethoxy-1-propanol	11.48 ± 0.69	22.42 ± 1.21 *
trans-3-Hexen-1-ol	2.89 ± 0.06	3.87 ± 0.31 *
1-Octanol	21.39 ± 3.08	40.16 ± 5.41 *
2,3-Butanediol	6.66 ± 0.38	7.00 ± 1.56
Benzyl alcohol	64.56 ± 1.00 *	55.79 ± 2.28
Phenylethyl alcohol	21,552.26 ± 318.76	21,573.65 ± 281.79
Tot Alcohols	**83,031.90**	**79,177.98**
Acids		
Acetic acid	502.93 ± 48.94	377.47 ± 13.25
Isobutyric acid	104.61 ± 0.54 *	76.38 ± 7.19
Propanoic acid	tr	5.16 ± 0.97 *
3-Methyl-butanoic acid (Isovaleric acid)	368.68 ± 2.67	333.23 ± 15.27
Hexanoic acid	516.36 ± 28.50	630.77 ± 4.40 *
Octanoic acid	772.13 ± 19.82	939.14 ± 13.97 *
n-Decanoic acid	60.41 ± 4.13	65.75 ± 15.09
Total Acids	**2325.12**	**2427.90**
Furan Compounds		
Furfural	tr	25.16 ± 0.18 *
γ-Butyrolactone	670.68 ± 4.95	503.76 ± 72.97
γ-Nonalactone (t)	18.60 ± 6.56	21.78 ± 1.62
5-Oxotetrahydrofuran-2-carboxylic acid (t)	91.71 ± 8.68	81.37 ± 5.32
Furan compound (t)	318.28 ± 3.25	316.93 ± 3.48
Total Furan Compounds	**1099.27**	**949.01**
Carbonyl Compounds		
Hexanal	10.79 ± 0.96	11.19 ± 0.23
3-Hydroxy-2-butanone (Acetoin)	9.69 ± 0.33	20.56 ± 1.01 *
Vanillin	27.02 ± 10.50	36.17 ± 4.81
Methyl vanillate	77.55 ± 8.62	74.78 ± 4.23
Ethyl vanillate	125.11 ± 11.24 *	63.72 ± 3.75
Total Carbonyl Compounds	**250.16** *	**206.42**
Other Compounds		
3-(Methylthio)-1-propanol	tr	6.62 ± 0.13 *
4-ethyl phenol	2.97 ± 0.05	3.38 ± 0.68
2,6-Dimethoxy-phenol (Syringol)	1.38 ± 0.14 *	tr
Total Other Compounds	**4.35**	**10.00** *

Data represent the means (± standard deviation) of the wine samples from 3 bottles. * = Asterisk in the row of each compound refer to significant differences (Tukey, $p < 0.05$). tr = trace; t = tentative identification.

vanillin. CO_2 wine shows higher levels of ethyl vanillate and syringol. These specific differences may affect sensory perception. For instance, furfural and vanillin are known to contribute to almond-like aromas (Yu et al., 2020), a typical sensory note of carbonic maceration wines (Tesniere & Flanzy, 2011).

Importantly, the absence of significant variation in 4-ethylphenol, suggests that maceration under N_2 does not increase the risk of spoilage by acetic acid bacteria and *Brettanomyces* yeasts, normally increased during classic CO_2 because of the higher pH, higher temperatures and absence of sulfur dioxide (Tesniere & Flanzy, 2011).

Based on these results, N_2 maceration may represent a valid alternative to classic CO_2 maceration, preserving the typical aroma of these wines.

3.5. Non-destructive evaluation

In the recent years, *E*-nose and NIR spectroscopy have been widely used for the analysis of grapes and wine. E-nose is used to detects volatile compounds by converting them into a detectable electric signals (Alfieri et al., 2024), while NIR spectroscopy is employed to assess wine composition, including reducing sugars, acids, phenolic compounds, among other metabolites (D. Cozzolino et al., 2006). Both instruments gives specific fingerprint-like patterns useful for prediction and discrimination purposes.

In this context, the k-means clustering analysis results from the E-nose show significant overlap between the CO_2 and N_2 samples. The two principal components explained 96.2 % of the total variance (62.8 % PC1 and 33.4 % for PC2) (Fig. 1). Although these components captured most of the variance, they did not result in a distinct separation between the two maceration treatments. This suggest that the aromatic differences between wines produced under CO_2 and N_2 atmospheres were not large enough for the E-nose to discriminate between them—an observation consistent with GC–MS results. Yet, the lack of clear separation in the E-nose data well reflect the analytical data of volatile profile where only small differences were observed. These small variations likely fall below the detection threshold of the E-nose used in this study. Hence, as previously reported, E-noses may have low selectivity, requiring advanced analytical methods to distinguish between similar compounds

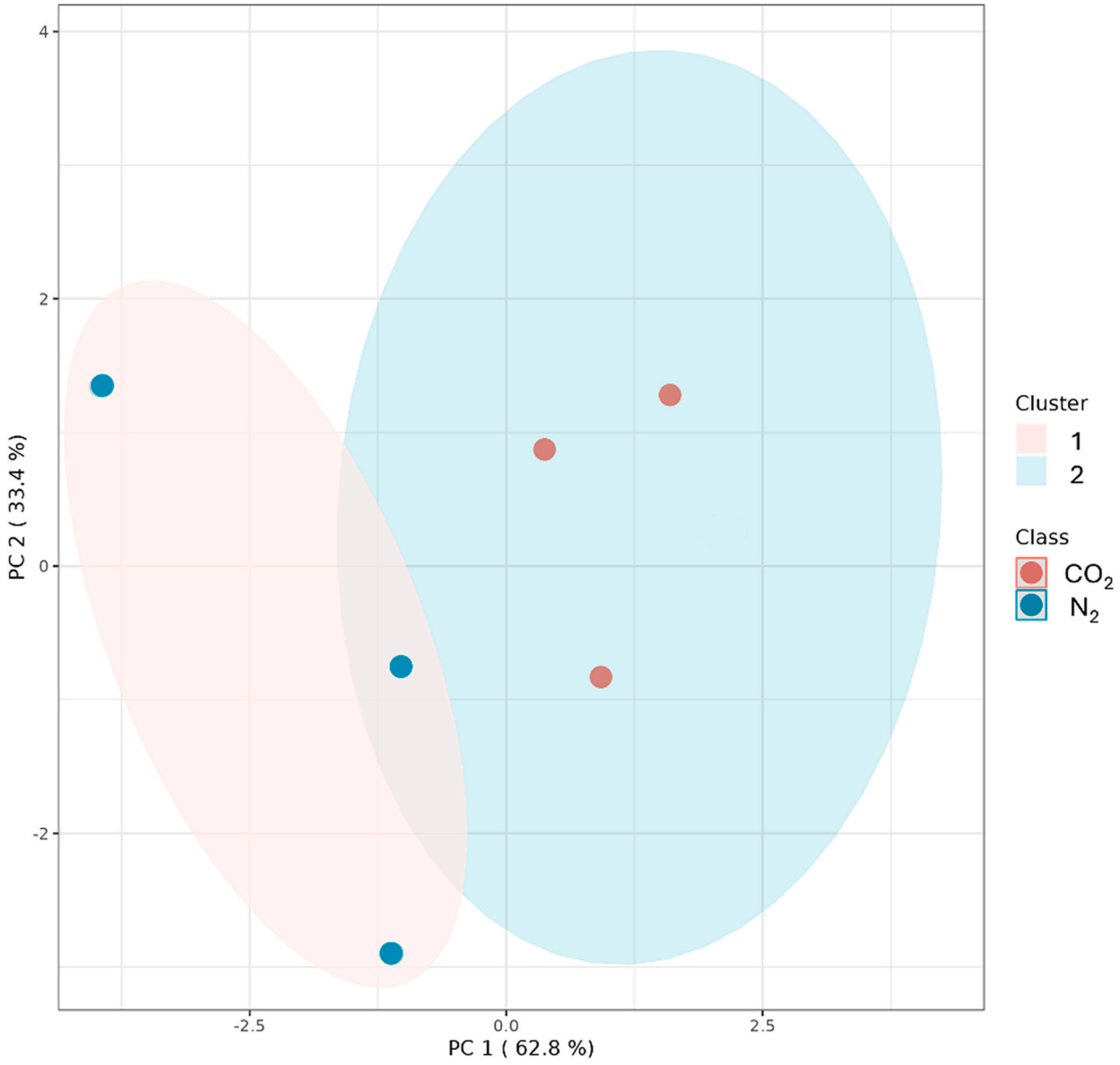

Fig. 1. K-means clustering results for the volatile profiles of wine samples produced with CO_2 (red) and N_2 (blue) maceration as detected by the E-nose. Data were normalized by autoscaling. (For interpretation of the references to colour in this figure legend, the reader is referred to the web version of this article.)

(Celdrán et al., 2022). Thus, integrating their use with traditional gas chromatography can give a more accurate information (Alfieri et al., 2024), especially when the difference in aromatic profile are not so remarkable.

In contrast, k-means clustering analysis of the NIR spectra revealed clear discrimination between wines macerated under CO_2 and N_2. The data are projected onto the first two principal components (PC1 and PC2), which together explain nearly the entirety of the variance (96.7 % and 3.1 %, respectively) (Fig. 2). The wines produced with CO_2 maceration are positioned distinctly along the positive side of PC1, while the wines made with N_2. maceration are located on the negative side. This separation indicates that the primary source of variance (PC1) effectively captures the chemical differences resulting from the two maceration gases. The clustering suggests that the choice of gas (CO_2 vs. N_2) during maceration has a measurable impact on the spectral features of the resulting wines. The small variance explained by PC2 (3.1 %) further indicates that secondary factors, such as slight experimental variations or minor differences in wine composition, may contribute to the separation, but they are less significant compared to the influence of the maceration gas.

Consistently, the NIR spectra reveal significant differences between the two acquisition. Fig. 3 shows the average spectra of the wines subjected to the different maceration. Both spectra exhibit similar absorption patterns, indicative of common wine components such as water, ethanol, organic acids and polyphenols (Anjos et al., 2022).

Although the overall shapes were quite similar, variations in absorbance intensity were observed in specific spectral ranges (1500–1850 nm), which may indicate slight differences in their internal composition.

For instance, the spectral region between 1450 and 1500 nm is associated with O—H bond vibrations, mainly related to water, ethanol, and organic acids, while the 1600–1800 nm range corresponds to combination bands of C—H and O—H bonds (Hu et al., 2018), which are characteristic of sugars, phenols, and ethanol (Daniel Cozzolino et al., 2008; Ferrer-Gallego et al., 2022). This hypothesis is well confirmed by the analytical measurement which highlighted significant differences between the two wines in polyphenols and anthocyanin fractions, as well as ethanol, glycerol and sugars.

It is important to note that K-means clustering was selected in this study because only two experimental groups were compared (CO_2 and N_2 maceration). In this context, the use of more complex multivariate classification methods would not have provided additional evidences, while a univariate approach would not have been appropriate for datasets of this nature, which are based on spectral fingerprints. K-means is particularly useful to evaluate whether distinct subgroups emerge within the sample clusters. In this regard, the results clearly reflect the behavior of the two analytical techniques: the *E*-nose did not detect any significant clustering, suggesting substantial overlap between treatments and confirming its low sensitivity to small differences in

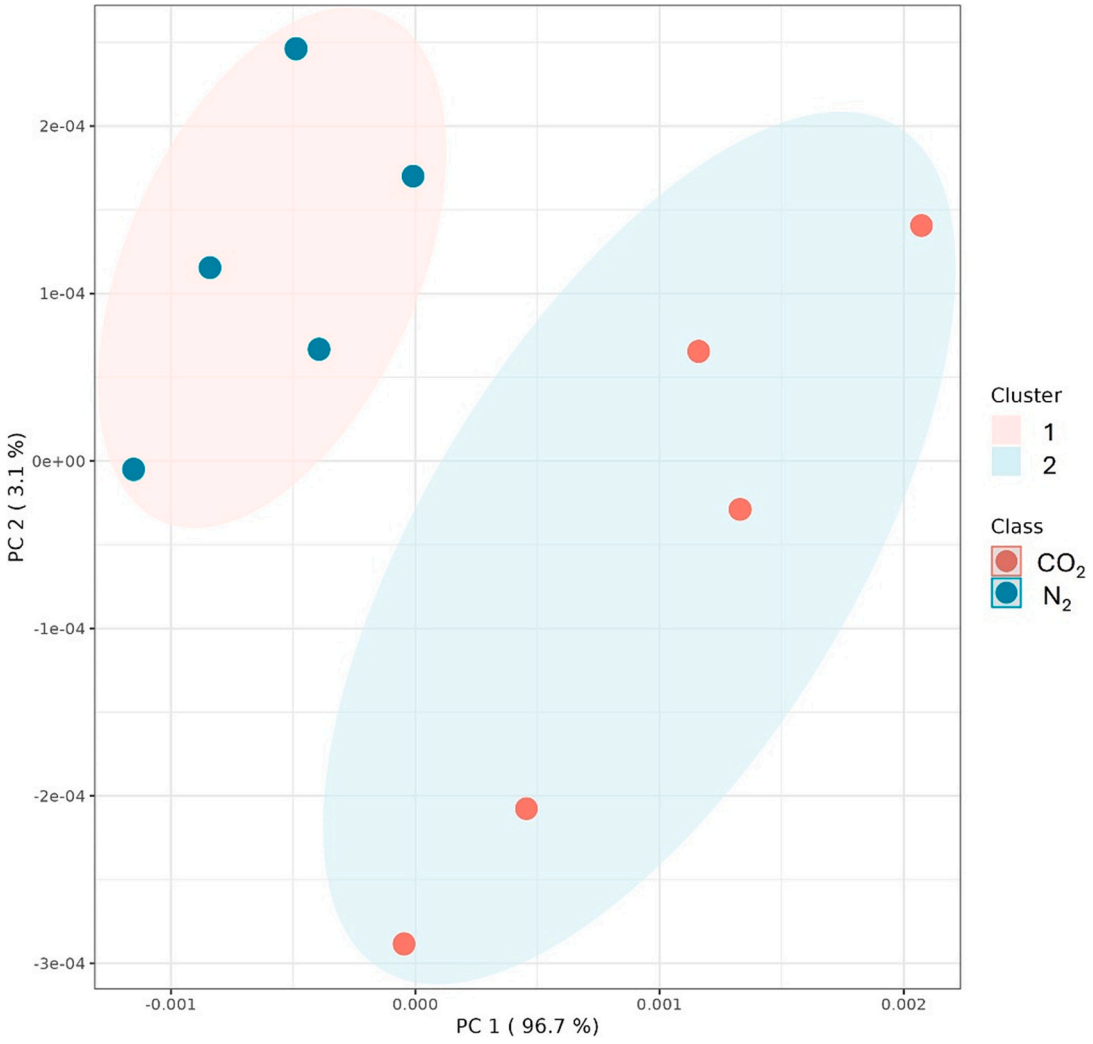

Fig. 2. K-means clustering results for the NIR spectral data (Abs = log 1/T) of wines macerated under CO_2 (red) and N_2 (blue) atmospheres. (For interpretation of the references to colour in this figure legend, the reader is referred to the web version of this article.)

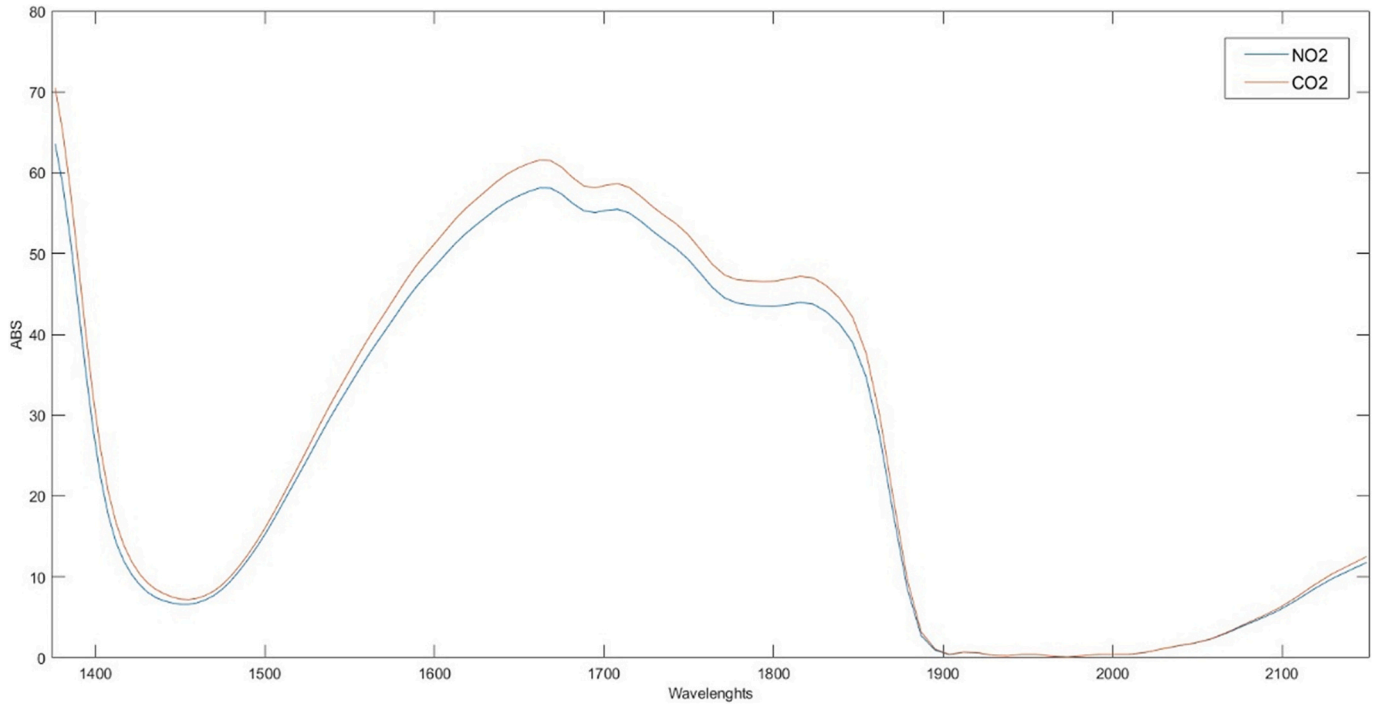

Fig. 3. Representative mean NIR spectra (Abs = log 1/T) of wine samples obtained after maceration under CO_2 and N_2 atmospheres.

volatile profiles. Conversely, the NIR data showed a clear separation between the two treatments, indicating a distinct impact of the maceration gas on wine composition. Moreover, while the NIR spectral fingerprint could be meaningfully interpreted by linking specific absorbance bands to chemical classes (e.g., water, ethanol, sugars, phenolics), the E-nose fingerprint remains more difficult to associate with specific volatile compounds, as current technology provides limited selectivity and compound-level resolution.

Overall, our results demonstrate the complementarity of non-destructive and traditional analytical techniques. While the E-nose alone showed limited resolution in this specific case, its output was coherent with GC–MS data, confirming the absence of strong volatile divergence. NIR spectroscopy, instead, effectively captured compositional differences, supporting its potential application as a rapid tool for monitoring treatment effects on wine during processing.

4. Conclusions

This study demonstrates that nitrogen maceration can serve as a viable alternative to carbonic maceration for producing high-quality red wines. The results confirmed the initial hypothesis: the use of different gases for inducing anoxia significantly influences metabolic processes, thus it is not only an oxygen deprivation. Specifically, from a compositional perspective, NM leads to enhanced polyphenol and anthocyanin extraction during maceration, likely due to differences in anaerobic metabolism compared to CO_2 atmospheres. HPLC analysis demonstrated that CO_2 maceration reduced flavonol and anthocyanin fractions, a trend confirmed by metabolomic analysis. Interestingly, nitrogen maceration appeared to stimulate anthocyanin production more efficiently, particularly simple anthocyanins, while CO_2 maceration favored an increase in acylated and coumaroylated anthocyanins.

On the other hand, although some minor differences were observed in VOCs profiles, the overall aroma remained comparable, suggesting that NM can preserve aromatic quality. Non-destructive techniques well reflected the chemical analyses: while the E-nose showed limited ability to differentiate between wines, very similar in their aromatic composition, NIR spectroscopy clearly captured the chemical distinctions between NM and CM wines. These results align with a growing interest in sustainable and innovative winemaking practices. Hence, nitrogen gas is widely available, non-toxic, and already used in wineries, simple produced by a membrane nitrogen generator of low cost, using filtered air. Carbon dioxide is low cost if produced by respiratory and fermentative metabolisms but it requires longer time. The use of gas CO_2 requires the purchase of tanks while the use of dry ice is costy and reduce the temperature of grapes slowing down the grape fermentation process. In both cases, if atmosphere is saturated with gas in an airtight cold room, precautions must be taken before opening the cold room door. CO_2 has the advantage is bacteriostatic thus reduces the potential fungi development while nitrogen is not. Thus the final suggestion, it is that the operator can start with nitrogen gas above all if it owns a nitrogen generator then leaving the CO_2 increasing thus arriving to an atmosphere almost 50–50 of the two gases.

CRediT authorship contribution statement

Alessandro Bianchi: Writing – review & editing, Writing – original draft, Visualization, Validation, Methodology, Investigation, Formal analysis, Data curation. **Severina Pacifico:** Writing – review & editing, Writing – original draft, Investigation, Formal analysis, Data curation. **Gregorio Santini:** Investigation, Formal analysis. **Stefano Pettinelli:** Writing – original draft, Investigation, Formal analysis, Data curation. **Gianmarco Alfieri:** Investigation, Formal analysis, Data curation. **Margherita Modesti:** Writing – review & editing, Writing – original draft, Methodology, Investigation, Formal analysis, Data curation. **Andrea Bellincontro:** Writing – original draft, Resources, Investigation, Formal analysis, Data curation. **Chiara Sanmartin:** Writing – original draft, Investigation, Formal analysis, Data curation. **Elisabetta Pittari:** Writing – original draft, Investigation, Formal analysis, Data curation. **Simona Piccolella:** Writing – original draft, Investigation, Formal analysis, Data curation. **Milena Petriccione:** Writing – review & editing, Writing – original draft, Visualization, Supervision, Resources, Investigation, Conceptualization. **Fabio Mencarelli:** Writing – review & editing, Writing – original draft, Visualization, Validation, Supervision, Resources, Conceptualization. **Paola Piombino:** Writing – review &

editing, Writing – original draft, Visualization, Validation, Supervision, Resources, Conceptualization.

Declaration of competing interest

The authors declare that they have no known competing financial interests or personal relationships that could have appeared to influence the work reported in this paper.

Acknowledgment

We would like to thank the SIAD Italia to have provided stainless steel tanks and gases

Appendix A. Supplementary data

Supplementary data to this article can be found online at https://doi.org/10.1016/j.foodchem.2025.144782.

Data availability

Data are available in the paper and in supplementary material

References

Alfieri, G., Modesti, M., Riggi, R., & Bellincontro, A. (2024). Recent advances and future perspectives in the E-nose technologies addressed to the wine industry. *Sensors, 24*(7), 2293. https://doi.org/10.3390/s24072293

Amarowicz, R., Carle, R., Dongowski, G., Durazzo, A., Galensa, R., Kammerer, D., … Piskula, M. K. (2009). Influence of postharvest processing and storage on the content of phenolic acids and flavonoids in foods. *Molecular Nutrition & Food Research, 53*(S2), S151–S183. https://doi.org/10.1002/mnfr.200700486

Anjos, O., Caldeira, I., Fernandes, T. A., Pedro, S. I., Vitória, C., Oliveira-Alves, S., … Canas, S. (2022). PLS-R calibration models for wine Spirit volatile phenols prediction by near-infrared spectroscopy. *Sensors, 22*(1), 286. https://doi.org/10.3390/s22010286

Antolini, A., Forniti, R., Modesti, M., Bellincontro, A., Catelli, C., & Mencarelli, F. (2021). First application of ozone postharvest fumigation to remove smoke taint from grapes. *Ozone: Science & Engineering, 43*(3), 254–262. https://doi.org/10.1080/01919512.2020.1796583

Bellincontro, A., Nicoletti, I., Valentini, M., Tomas, A., De Santis, D., Corradini, D., & Mencarelli, F. (2009). Integration of nondestructive techniques with destructive analyses to study postharvest water stress of winegrapes. *American Journal of Enology and Viticulture, 60*(1), 57–65.

Bianchi, A., Pettinelli, S., Pittari, E., Paoli, L., Sanmartin, C., Pons, A., … Piombino, P. (2025). Accelerated oxygenation for the production of fortified (mystelle-type) sweet wines: Effects on the chemical and flavor profile. *Journal of the Science of Food and Agriculture, 105*(3), 2021–2031. https://doi.org/10.1002/jsfa.13978

Bianchi, A., Pettinelli, S., Santini, G., Taglieri, I., Zinnai, A., Petriccione, M., … Bellincontro, A. (2024). Postharvest wine grape dehydration: Ethanol dissipation from grape and biochemical changes. *Journal of the Science of Food and Agriculture, 104*(3), 1591–1598. https://doi.org/10.1002/jsfa.13042

Bianchi, A., Santini, G., Piombino, P., Pittari, E., Sanmartin, C., Moio, L., Modesti, M., Bellincontro, A., & Mencarelli, F. (2023). Nitrogen maceration of wine grape: An alternative and sustainable technique to carbonic maceration. *Food Chemistry, 404*, Article 134138. https://doi.org/10.1016/j.foodchem.2022.134138

Bianchi, A., Taglieri, I., Rimbotti Antinori, V., Palla, F., Macaluso, M., Ferroni, G., Sanmartin, C., Venturi, F., & Zinnai, A. (2021). A statistical approach to describe the ripening evolution of sangiovese grapes coming from different chianti classico sub-areas. *Foods, 10*(10), 2292. https://doi.org/10.3390/foods10102292

Bloom, A. J. (2015). Photorespiration and nitrate assimilation: A major intersection between plant carbon and nitrogen. *Photosynthesis Research, 123*(2), 117–128. https://doi.org/10.1007/s11120-014-0056-y

Cameleyre, M., Lytra, G., Tempere, S., & Barbe, J.-C. (2015). Olfactory impact of higher alcohols on red wine fruity Ester aroma expression in model solution. *Journal of Agricultural and Food Chemistry, 63*(44), 9777–9788. https://doi.org/10.1021/acs.jafc.5b03489

Castellarin, S. D., Matthews, M. A., Di Gaspero, G., & Gambetta, G. A. (2007). Water deficits accelerate ripening and induce changes in gene expression regulating flavonoid biosynthesis in grape berries. *Planta, 227*(1), 101–112. https://doi.org/10.1007/s00425-007-0598-8

Celdrán, A. C., Oates, M. J., Molina Cabrera, C., Pangua, C., Tardaguila, J., & Ruiz-Canales, A. (2022). Low-cost electronic nose for wine variety identification through machine learning algorithms. *Agronomy, 12*(11), 2627. https://doi.org/10.3390/agronomy12112627

Chidi, B. S., Bauer, F. F., & Rossouw, D. (2018). Organic acid metabolism and the impact of fermentation practices on wine acidity - a review. *South African Journal of Enology and Viticulture, 39*(2), 315–329. https://doi.org/10.21548/39-2-3172

Cho, H.-Y., Loreti, E., Shih, M.-C., & Perata, P. (2021). Energy and sugar signaling during hypoxia. *New Phytologist, 229*(1), 57–63. https://doi.org/10.1111/nph.16326

Cozzolino, D., Dambergs, R. G., Janik, L., Cynkar, W. U., & Gishen, M. (2006). Analysis of grapes and wine by near infrared spectroscopy. *Journal of Near Infrared Spectroscopy, 14*(5), 279–289. https://doi.org/10.1255/jnirs.679

Cozzolino, D., Cynkar, W. U., Dambergs, R. G., Mercurio, M. D., & Smith, P. A. (2008). Measurement of condensed tannins and dry matter in red grape homogenates using near infrared spectroscopy and partial least squares. *Journal of Agricultural and Food Chemistry, 56*(17), 7631–7636. https://doi.org/10.1021/jf801563z

Di Natale, C., Paolesse, R., & D'Amico, A. (2007). Metalloporphyrins based artificial olfactory receptors. *Sensors and Actuators, B: Chemical, 121*(1), 238–246. https://doi.org/10.1016/j.snb.2006.09.038

Ferreira, V., de la Fuente, A., & Sáenz-Navajas, M. P. (2022). Wine aroma vectors and sensory attributes. In A. G. Reynolds (Ed.), *Managing wine quality* (pp. 3–39). Sawston, UK: Woodhead Publishing. https://doi.org/10.1016/B978-0-08-102067-8.00008-7.

Ferrer-Gallego, R., Rodríguez-Pulido, F. J., Toci, A. T., & García-Estevez, I. (2022). Phenolic composition, quality and authenticity of grapes and wines by vibrational spectroscopy. *Food Reviews International, 38*(5), 884–912. https://doi.org/10.1080/87559129.2020.1752231

Formato, M., Vastolo, A., Piccolella, S., Calabrò, S., Cutrignelli, M. I., Zidorn, C., & Pacifico, S. (2022a). Antioxidants in animal nutrition: UHPLC-ESI-QqTOF analysis and effects on in vitro rumen fermentation of oak leaf extracts. *Antioxidants, 11*(12), 2366. https://doi.org/10.3390/antiox11122366

Formato, M., Vastolo, A., Piccolella, S., Calabrò, S., Cutrignelli, M. I., Zidorn, C., & Pacifico, S. (2022b). *Castanea sativa* mill. Leaf: UHPLC-HR MS/MS analysis and effects on in vitro rumen fermentation and Methanogenesis. *Molecules, 27*(24), Article 8662. https://doi.org/10.3390/molecules27248662

Gawel, R., Schulkin, A., Smith, P. A., Espinase, D., & McRae, J. M. (2020). Effect of dissolved carbon dioxide on the sensory properties of still white and red wines. *Australian Journal of Grape and Wine Research, 26*(2), 172–179. https://doi.org/10.1111/ajgw.12429

Giacosa, S., Ferrero, L., Paissoni, M. A., Río Segade, S., Gerbi, V., & Rolle, L. (2023). Grape skin anthocyanin extraction from red varieties during simulated maceration: Influence of grape seeds and pigments adsorption on their surface. *Food Chemistry, 424*, Article 136463. https://doi.org/10.1016/j.foodchem.2023.136463

Gibbs, J., & Greenway, H. (2003). Review: Mechanisms of anoxia tolerance in plants. I. Growth, survival and anaerobic catabolism. *Functional Plant Biology, 30*(1), 1–47. https://doi.org/10.1071/PP98095

Guan, L., Dai, Z., Wu, B.-H., Wu, J., Merlin, I., Hilbert, G., Renaud, C., Gomès, E., Edwards, E., Li, S.-H., & Delrot, S. (2016). Anthocyanin biosynthesis is differentially regulated by light in the skin and flesh of white-fleshed and teinturier grape berries. *Planta, 243*(1), 23–41. https://doi.org/10.1007/s00425-015-2391-4

Hammer, Ø., Harper, D. A. T., & Ryan, P. D. (2001). Past: Paleontological statistics software package for education and data analysis. Palaeontologia. *Palaeontologia Electronica, 4*(1), 9. http://palaeo-electronica.org/2001_1/past/issue1_01.htm.

Hu, L., Yin, C., Ma, S., & Liu, Z. (2018). Rapid detection of three quality parameters and classification of wine based on Vis-NIR spectroscopy with wavelength selection by ACO and CARS algorithms. *Spectrochimica Acta Part A: Molecular and Biomolecular Spectroscopy, 205*, 574–581. https://doi.org/10.1016/j.saa.2018.07.054

Imahori, Y. (2024). Controlled atmosphere storage for fruits and vegetables. In S. Ali, S. A. Mir, B. N. Dar, & S. Ejaz (Eds.), *Sustainable postharvest Technologies for Fruits and Vegetables* (1st ed., pp. 65–85). Boca Raton, FL, USA: CRC Press. https://doi.org/10.1201/9781003370376-5.

Jiménez, J. B., Orea, J. M., Ureña, A. G., Escribano, P., De La Osa, P. L., & Guadarrama, A. (2007). Short anoxic treatments to enhance trans-resveratrol content in grapes and wine. *European Food Research and Technology, 224*(3), 373–378. https://doi.org/10.1007/s00217-006-0329-6

Karn, A., Diaz-Garcia, L., Reshef, N., Zou, C., Manns, D. C., Cadle-Davidson, L., … Sacks, G. L. (2021). The genetic basis of anthocyanin acylation in north American grapes (*Vitis* spp.). *Genes, 12*(12), Article 1962. https://doi.org/10.3390/genes12121962

Ke, D., Yahia, E., Hess, B., Zhou, L., & Kader, A. A. (1995). Regulation of fermentative metabolism in avocado fruit under oxygen and carbon dioxide stresses. *Journal of the American Society for Horticultural Science, 120*(3), 481–490. https://doi.org/10.21273/jashs.120.3.481

Littarru, E., Modesti, M., Alfieri, G., Pettinelli, S., Floridia, G., Bellincontro, A., Sanmartin, C., & Brizzolara, S. (2025). Optimizing the winemaking process: NIR spectroscopy and e-nose analysis for the online monitoring of fermentation. *Journal of the Science of Food and Agriculture, 105*(3), 1465–1475. https://doi.org/10.1002/jsfa.13336

Maoz, I., De Rosso, M., Kaplunov, T., Vedova, A. D., Sela, N., Flamini, R., … Lichter, A. (2019). Metabolomic and transcriptomic changes underlying cold and anaerobic stresses after storage of table grapes. *Scientific Reports, 9*(1), 2917. https://doi.org/10.1038/s41598-019-39253-8

Martínez-García, R., Moreno, J., Bellincontro, A., Centioni, L., Puig-Pujol, A., Peinado, R. A., … García-Martínez, T. (2021). Using an electronic nose and volatilome analysis to differentiate sparkling wines obtained under different conditions of temperature, ageing time and yeast formats. *Food Chemistry, 334*(June 2020), Article 127574. https://doi.org/10.1016/j.foodchem.2020.127574

Mastrangelo, N., Bianchi, A., Pettinelli, S., Santini, G., Merlani, G., Bellincontro, A., … Mencarelli, F. (2023). Novelty of Italian grape ale (IGA) beer: Influence of the addition of Gamay macerated grape must or dehydrated Aleatico grape pomace on the aromatic profile. *Heliyon, 9*(10), Article e20422. https://doi.org/10.1016/j.heliyon.2023.e20422

Modesti, M., Alfieri, G., Chieffo, C., Mencarelli, F., Vannini, A., Catalani, A., Chilosi, G., & Bellincontro, A. (2024). Destructive and non-destructive early detection of postharvest noble rot (*Botrytis cinerea*) in wine grapes aimed at producing high-quality wines. *Journal of the Science of Food and Agriculture, 104*(4), 2314–2325. https://doi.org/10.1002/jsfa.13120

Páscoa, R. N. M. J., Porto, P. A. L. S., Cerdeira, A. L., & Lopes, J. A. (2020). The application of near infrared spectroscopy to wine analysis: An innovative approach using lyophilization to remove water bands interference. *Talanta, 214*, Article 120852. https://doi.org/10.1016/j.talanta.2020.120852

Paul, V., & Pandey, R. (2014). Role of internal atmosphere on fruit ripening and storability—A review. *Journal of Food Science and Technology, 51*(7), 1223–1250. https://doi.org/10.1007/s13197-011-0583-x

Pettinelli, S., Alfieri, G., Bianchi, A., Baris, F., Chinnici, F., Mencarelli, F., … Modesti, M. (2025). Fortified or passito sweet wines from Aleatico grapes subjected to different dehydration conditions: Chemical and aromatic profile using destructive and non-destructive analyses. *OENO one, 59*(1). https://doi.org/10.20870/oeno-one.2025.59.1.8372

Pettinelli, S., Alfieri, G., Bianchi, A., Uliva, A., Floridia, G., Bellincontro, A., & Mencarelli, F. (2024). Use of AirMixing M.I.® resonance waves to produce aroma richer Sangiovese wine without sulphites addition in a sustainable way. *LWT, 198* (April), Article 116075. https://doi.org/10.1016/j.lwt.2024.116075

Pettinelli, S., Pardini, L., De Angeli, G., Bianchi, A., Najar, B., Cerreta, R., … Mencarelli, F. (2022). Innovative "soft" maceration techniques in red grape fermentation. *Beverages, 8*(4), 62. https://doi.org/10.3390/beverages8040062

Pfister-Sieber, M., & Brändle, R. (1994). Aspects of plant behaviour under anoxia and post-anoxia. *Proceedings of the Royal Society of Edinburgh. Section B. Biological Sciences, 102*, 313–324. https://doi.org/10.1017/S0269727000014305

Piombino, P., Moio, L., & Genovese, A. (2019). Orthonasal vs. retronasal: Studying how volatiles' hydrophobicity and matrix composition modulate the release of wine odorants in simulated conditions. *Food Research International, 116*, 548–558. https://doi.org/10.1016/j.foodres.2018.08.072

Revilla, E., Arroyo-Garcia, R., Bellido, A., Carrasco, D., Puig, A., & Ruiz-Garcia, L. (2017). Fingerprints of anthocyanins and Flavonols in Wild grapes (*Vitis vinifera* L. ssp. *sylvestris* (Gmelin) Hegi). In A. M. Jordão, & F. Cosme (Eds.), *Grapes and wines - advances in production, processing, analysis and valorization* (p. 5772). Rijeka, Croatia: IntechOpen. https://doi.org/10.5772/intechopen.70861.

Rinaldo, A. R., Cavallini, E., Jia, Y., Moss, S. M. A., McDavid, D. A. J., Hooper, L. C., … Walker, A. R. (2015). A grapevine anthocyanin acyltransferase, transcriptionally regulated by VvMYBA, can produce Most Acylated anthocyanins present in grape skins. *Plant Physiology, 169*(3), 1897–1916. https://doi.org/10.1104/pp.15.01255

Rouxinol, M. I., Martins, M. R., Barroso, J. M., & Rato, A. E. (2023). Wine grapes ripening: A review on climate effect and analytical approach to increase wine quality. *Applied Biosciences, 2*(3), 347–372. https://doi.org/10.3390/applbiosci2030023

Rouxinol, M. I., Martins, M. R., Murta, G. C., Mota Barroso, J., & Rato, A. E. (2022). Quality assessment of red wine grapes through NIR spectroscopy. *Agronomy, 12*(3), 637. https://doi.org/10.3390/agronomy12030637

Ruiz-Capillas, C., & Moral, A. (2001). Residual effect of CO2 on hake (*Merluccius merluccius* L.) stored in modified and controlled atmospheres. *European Food Research and Technology, 212*(4), 413–420. https://doi.org/10.1007/s002170000270

Salvatierra, A., Toro, G., Mateluna, P., Opazo, I., Ortiz, M., & Pimentel, P. (2020). Keep calm and survive: Adaptation strategies to energy crisis in fruit trees under root hypoxia. *Plants, 9*(9), 1108. https://doi.org/10.3390/plants9091108

San-Juan, F., Ferreira, V., Cacho, J., & Escudero, A. (2011). Quality and aromatic sensory descriptors (mainly fresh and dry fruit character) of Spanish red wines can be predicted from their aroma-active chemical composition. *Journal of Agricultural and Food Chemistry, 59*(14), 7916–7924. https://doi.org/10.1021/jf1048657

Santini, G., Bianchi, A., Pettinelli, S., Modesti, M., Cerreta, R., & Bellincontro, A. (2023). Air speed and plastic crate vent-holes for wine grape quality during postharvest dehydration: Commercial and laboratory studies. *Journal of the Science of Food and Agriculture, 103*, 7293–7301. https://doi.org/10.1002/jsfa.12817

Santonico, M., Bellincontro, A., De Santis, D., Di Natale, C., & Mencarelli, F. (2010). Electronic nose to study postharvest dehydration of wine grapes. *Food Chemistry, 121* (3), 789–796. https://doi.org/10.1016/j.foodchem.2009.12.086

Sun, J., Lin, L., & Chen, P. (2012). Study of the mass spectrometric behaviors of anthocyanins in negative ionization mode and its applications for characterization of anthocyanins and non-anthocyanin polyphenols. *Rapid Communications in Mass Spectrometry, 26*(9), 1123–1133. https://doi.org/10.1002/rcm.6209

Tarì, U., Pettinelli, S., Bianchi, A., Pollon, M., Alfieri, G., Vitaggio, C., … Mencarelli, F. (2024). Identifying wine grape aromatic maturity using e-nose and GC-MS: The case of Nerello Mascalese grapes from two contrade of the Etna area. *OENO one, 58*(1). https://doi.org/10.20870/oeno-one.2024.58.1.7752

Tesniere, C., & Abbal, P. (2009). Alcohol Dehydrogenase Genes & Proteins In Grapevine. In K. A. Roubelakis-Angelakis (Ed.), *Grapevine Molecular Physiology & Biotechnology* (pp. 141–160). Netherlands, Dordrecht, The Netherlands: Springer. https://doi.org/10.1007/978-90-481-2305-6_6.

Tesniere, C., & Flanzy, C. (2011). Carbonic maceration wines: Characteristics and winemaking process. In (1st ed.), *Vol. 63. Advances in food and nutrition research*. Elsevier Inc.. https://doi.org/10.1016/B978-0-12-384927-4.00001-4

Tesniere, C., Pradal, M., El-Kereamy, A., Torregrosa, L., Chatelet, P., Roustan, J. P., & Chervin, C. (2004). Involvement of ethylene signalling in a non-climacteric fruit: New elements regarding the regulation of ADH expression in grapevine. *Journal of Experimental Botany, 55*(406), 2235–2240. https://doi.org/10.1093/jxb/erh244

Unusan, N. (2020). Proanthocyanidins in grape seeds: An updated review of their health benefits and potential uses in the food industry. *Journal of Functional Foods, 67*, Article 103861. https://doi.org/10.1016/j.jff.2020.103861

Verdenal, T., Dienes-Nagy, Á., Spangenberg, J. E., Zufferey, V., Spring, J.-L., Viret, O., … van Leeuwen, C. (2021). Understanding and managing nitrogen nutrition in grapevine: A review. *OENO one, 55*(1), 1–43. https://doi.org/10.20870/oeno-one.2021.55.1.3866

Viana, E. S., Gomide, L. A. M., & Vanetti, M. C. D. (2005). Effect of modified atmospheres on microbiological, color and sensory properties of refrigerated pork. *Meat Science, 71*(4), 696–705. https://doi.org/10.1016/j.meatsci.2005.05.013

Waterhouse, A. L., Price, S. F., McCord, J. D. B. T.-M., & in E.. (1999). [11] reversed-phase high-performance liquid chromatography methods for analysis of wine polyphenols. In L. Packer (Ed.), *Vol. 299. Oxidants and antioxidants part a* (pp. 113–121). Cambridge, MA, USA: Academic Press. https://doi.org/10.1016/S0076-6879(99)99014-6.

de Wild, H. P. J., Otma, E. C., & Peppelenbos, H. W. (2003). Carbon dioxide action on ethylene biosynthesis of preclimacteric and climacteric pear fruit. *Journal of Experimental Botany, 54*(387), 1537–1544. https://doi.org/10.1093/jxb/erg159

Wongs-Aree, C., & Noichinda, S. (2018). Glycolysis fermentative by-products and secondary metabolites involved in plant adaptation under hypoxia during pre- and postharvest. In K. K. Das, & M. S. Biradar (Eds.), *Hypoxia and anoxia* (pp. 59–72). Rijeka, Croatia: IntechOpen. https://doi.org/10.5772/intechopen.80226.

Xiao, Z., Liao, S., Rogiers, S. Y., Sadras, V. O., & Tyerman, S. D. (2018). Effect of water stress and elevated temperature on hypoxia and cell death in the mesocarp of shiraz berries. *Australian Journal of Grape and Wine Research, 24*(4), 487–497. https://doi.org/10.1111/ajgw.12363

Xiao, Z., Rogiers, S. Y., Sadras, V. O., & Tyerman, S. D. (2018). Hypoxia in grape berries: The role of seed respiration and lenticels on the berry pedicel and the possible link to cell death. *Journal of Experimental Botany, 69*(8), 2071–2083. https://doi.org/10.1093/jxb/ery039

Yousuf, P. Y., Shabir, P. A., & Hakeem, K. R. (2022). In P. Y. Yousuf, P. A. Shabir, & K. R. Hakeem (Eds.), *Advances in plant nitrogen metabolism* (1st ed.). Boca Raton, FL, USA: CRC Press. https://doi.org/10.1201/9781003248361.

Yu, H., Xie, T., Xie, J., Chen, C., Ai, L., & Tian, H. (2020). Aroma perceptual interactions of benzaldehyde, furfural, and vanillin and their effects on the descriptor intensities of Huangjiu. *Food Research International, 129*, Article 108808. https://doi.org/10.1016/j.foodres.2019.108808